Joining of Silicon Nitride to Metals or Alloys Using Amorphous Cu-Ti Filler Metal†

Masaaki NAKA*, Tasuku TANAKA*** and Ikuo OKAMOTO**

Abstract

Silicon nitride has been joined with various metals and alloys using amorphous $Cu_{50}Ti_{50}$ filler alloy. The amorphous filler alloy in width of about 1 cm and thickness of about 45 μm was produced by rapid quenching of the liquid alloy.

Under vacuum condition at 1000°C for 5 min Si_3N_4 was joined with iron or copper, and super inver, inver, kovar or SUS 304 alloy. During brazing, Ti in Cu-Ti filler reacts with Si_3N_4 and Fe, Cu or Co dissolves from metal or alloy to the filler. In the case of joining with copper large amounts of copper dissolve into the filler and the titanium in the filler diffuses into copper.

The joining strength of Si_3N_4 with metal or alloy decreases with an increase in the thermal expansion coefficient or the product of thermal expansion coefficient and elastic modulus of metal and alloy. The thermal stress that arises from the difference of thermal expansion coefficoent of ceramic and metal or alloy affects the joining strength of ceramic and metal. In particular, the tension stress in the perpendicular direction to the joining interface takes place at the tension-tension stress region in the ceramic near the edge of metal or alloy.

KEY WORDS: (Brazing) (Joining) (Ceramics) (Nitride) (Silicon Nitride) (Amorphous Titanium Filler) (Amorphous Filler Metal) (Kovar) (Super Invar) (Invar) (Copper) (Stainless Steel)

1. Introduction

An increasing interest has been focused on ceramics as structural components because of their superior heat-resistance and adhesion-resistance. Silicon nitride (Si_3N_4) that is composed of cobalent bondings possesses excellent mechanical properties, compared with oxide ceramics that is composed of ionic bondings. Ceramics is made in relatively simple shapes, and the fabrication of more complex shapes and the inherent brittleness of ceramics requires the joining of ceramics to metals in practical applications.

Although some efforts have been expended in joining of oxide ceramics to metals[1,2] satisfactory studies of joining of non-oxide ceramics to metal, in particular silicon nitride to metals, have not yet reported.

It is the purpose of this paper to join Si_3N_4 to metals or alloys using amorphous Cu-Ti alloy filler, which adds the simplicity and reliability to the joining method[2], and further to make clear the joining mechanism.

2. Experimentals

$Cu_{50}Ti_{50}$ alloy filler containing 50 at% Ti was produced by rapid quenching of the liquid alloy, where the number attached to the filler designates the atomic percent. The liquid alloy of desired composition which was first prepared by argon arc melting was ejected onto the outer surface of a rapidly rotating wheel. The diameter of wheel used is 20 cm. The amorphous filler produced is about 1 cm wide and about 45 μm thick. **Fig. 1** shows the schematic of quenching apparatus. The diffraction pattern of $Cu_{50}Ti_{50}$ filler with $Cu{\cdot}K_\alpha$ raddiation is shown in **Fig. 2** which includes that of the crystalline alloy. The amorphous alloy provides the diffused X-ray diffraction pattern that is simillar to liquid metal, since the alloy posseses no atomic regularity in long range order. The amorphous alloy filler containing the high titanium content exhibits the superior flexibility, and can be bent to the encounter side and punched out to the desired size. These add simlicity to the joining method.

Si_3N_4 used is sintered at ordinary pressured, which contains a few weight percent of Al_2O_3 as sintering aid, and other impuities of Y, Fe and W (produced by Kyoto Ceramic Co., Ltd.). Metals and Alloys are iron, copper, Super Invar (32wt%Ni, 17wt%Co, bal. Fe), Invar 64wt%Fe, 36wt%Ni), Kovar (29wt%Ni, 17wt%Co, balFe)

† Received on 31, October, 1985.

* Associate Professor
** Professor
*** Graduate Student of Osaka University (Present address, Hitachi Co. Ltd.)

Transactions of JWRI is published by Welding Research Institute of Osaka University, Ibaraki, Osaka 567, Japan

and SUS304. Other materials used are Al_2O_3, ZrO_2 (5.5 wt%CaO) and MgO.

Metal or ally of 6 mm diameter and 3 mm thickness, and Si_3N_4 of 15 mm diameter and 3 mm thickness were used to make a lap joint using amorphous $Cu_{50}Ti_{50}$ filler of 6 mm diameter and 45 μm thickness as shown in **Fig. 3**. The brazing condition is 1000°C above 25°C from the melting point of the filler for 5 min in 1×10^{-5} torr. The heating rate up to brazing temperature was 20°C/min and the cooling rate after brazing was 19°C/min down to 600°C and then about 1°C/min down to room temperature. The joining strength of the lap joint was determined by fracture shear loading using a cross head speed of 1 mm/min at room temperature. The microstructures and element distribution of specimens joined were determined by means of scanning electron microscope and EDX microanalyser, respectively.

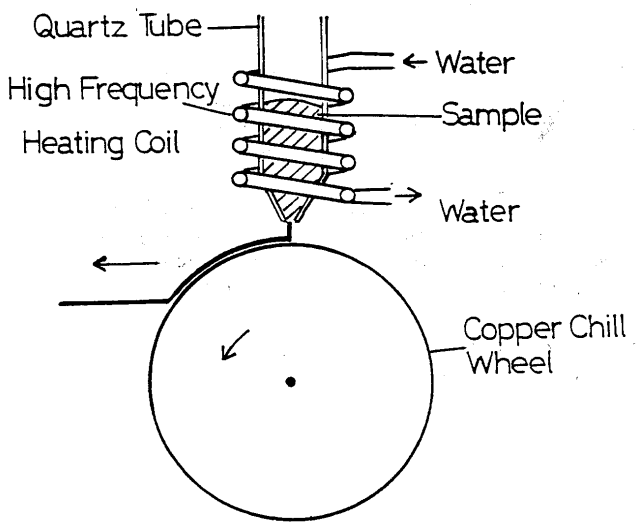

Fig. 1 Schematic of rapid quenching apparatus.

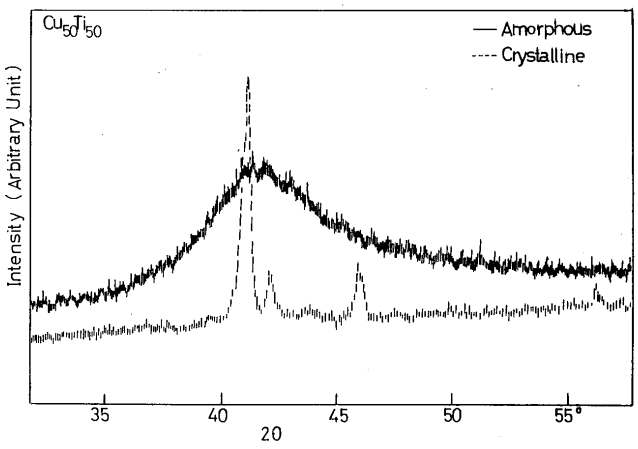

Fig. 2 X-ray diffraction pattern of $Cu_{50}Ti_{50}$ amorphous filler.

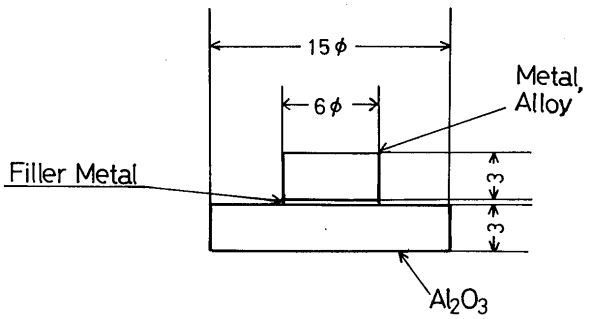

Fig. 3 Joint of Si_3N_4 and metal or alloy using amorphous filler.

3. Results

In order to suppress the dissolution of metals or alloys into the filler, the joining temperature was 1000°C above 25°C above the melting point of the filler. The joining strength of Si_3N_4/metal or alloy, and Si_3N_4/oxide ceramic joints, and elastic moduli and thermal expansion coefficients of materials are shown in **Table 1**. The joining strength of Si_3N_4/metal or alloy is large for Super Invar alloy which posseses the small expansion coefficient ($\alpha = 1.3 \times 10^{-6}$/°C) and small for Cu which posseses the large expansion coefficient ($\alpha = 17.2 \times 10^{-6}$/°C). These facts indicate that the joining strength is related to the thermal expansion coefficient of metals and alloys. Thus, the joining strength is plotted against the thermal expansion coefficient of metal or alloy in **Fig. 4**. The joining strength decreases with an increase in α, that is, an increase in strain occured in the joint. The figure 4 also includes

Table 1 Joining strength of Si_3N_4/metal or alloy and Si_3N_4/oxide ceramic joint and elastic modulus and thermal expansion coefficient of material.

Materials	Joining strength (kgf/mm²)	Elastic modulus (×10³ kgf/mm²)	Thermal expansion coefficient (×10⁻⁶/°C)
Fe	13.8	21	12.1 (10-200°C)
Cu	1.5	11.2	17.2 (0-200°C)
Super Invar	19.8	15	1.3 (30-100°C)
Invar	9.7	15	2.0 (30-100°C)
Kovar	3.5	15	6.0 (30-500°C)
SUS 304	9.3	21	17.8 (0 -300°C)
Al_2O_3	1.0	36.7	8.1 (25°C)
ZrO_2	0	13.4	10.0(25°C)
MgO	0	8.7	13.3(25°C)
Si_3N_4	–	30	3.7(40-800°C)

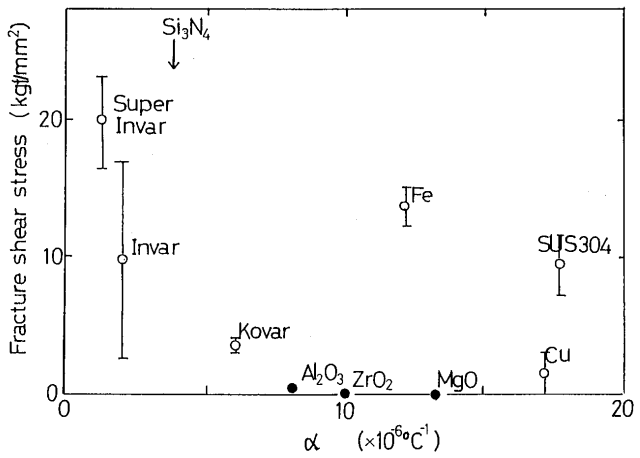

Fig. 4 Fracture shear stress of Si_3N_4/metal or alloy and Si_3N_4/oxide ceramic plotted against thermal expansion coefficient α of material.

the joining strength of Si_3N_4 to oxide ceramics. The thermal stress which arose from the difference during cooling broke the joint of Si_3N_4 to ZrO_2 or MgO at the interface between and the filler. **Fig. 5** shows that the strength decreases with an increase in $\alpha \cdot E$, where E is the elastic modulus of metal, alloy or oxide ceramic. $\alpha \cdot E$ is related with the thermal stress during cooling after brazing.

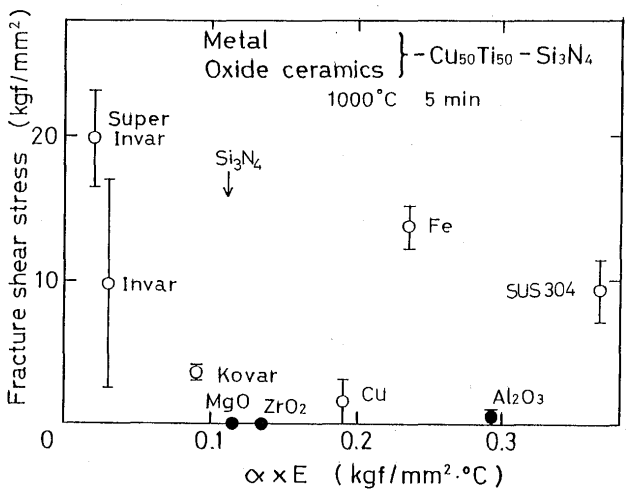

Fig. 5 Fracture shear stress of Si_3N_4/metal or alloy and Si_3N_4/oxide ceramic plotted against $\alpha \cdot E$, where α and E are the thermal expansion coefficient and elastic modulus of materials, respectively.

3.2 Mirostructures at the joint interface

Fig. 6 shows the microstructures of joints of Si_3N_4 and Fe, Cu, SUS304, Kovar, Invar and Super Invar alloys. The Cu-Ti filler wets well ceramics, metals and alloys. No defects and voids are formed at the interface of joints. The filler used is observed in Si_3N_4/metal or alloy joint except for Si_3N_4/Cu joint. In Si_3N_4/Cu joint copper dissolves into the Cu-Ti filler and the filler extends into copper. While copper possesses the almost same thermal expansion coefficient as SUS304, the joining strength of Si_3N_4/Cu joint is smaller than that of Si_3N_4/SUS304 joint.

Figs. 7 and **8** show SEM microstructures and EDX spot analyses for Ti, Si, Cu and Fe at the interface between Si_3N_4 and Fe, respectively. In Fig. 7 Ti peak corresponds to TiN formed at the interface between Si_3N_4 and Cu-Ti filler. TiN is formed by the reaction of $Si_3N_4 + 4Ti = 4TiN + 3Si$[3], and the separated Si reacts with Ti and Cu to form silicides. The spot analyses of (i), (ii) and (iii) in Fig. 8 indicate that Fe dissolves into silicides, and Fe-Ti intermetallic compound is formed at the interface on iron side. TiN possesses the suitable thermal expansion coefficient to relax the thermal stress took place during cooling, because its α is the intermediate value between $\alpha = 12.1 \times 10^{-6}/°C$ for iron and $\alpha = 3.7 \times 10^{-6}/°C$ for Si_3N_4.[4]

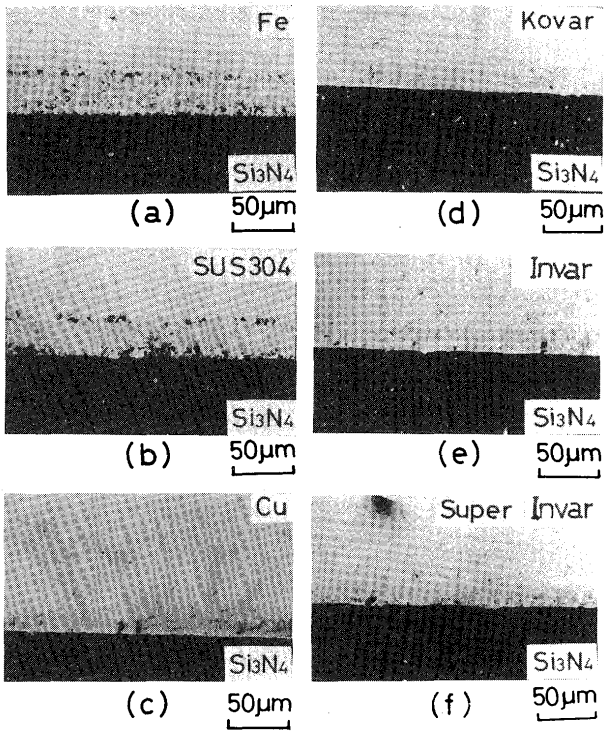

Fig. 6 Microphotographs of the interface of Si_3N_4 and metal or alloy brazed at 1000°C for 5 min.

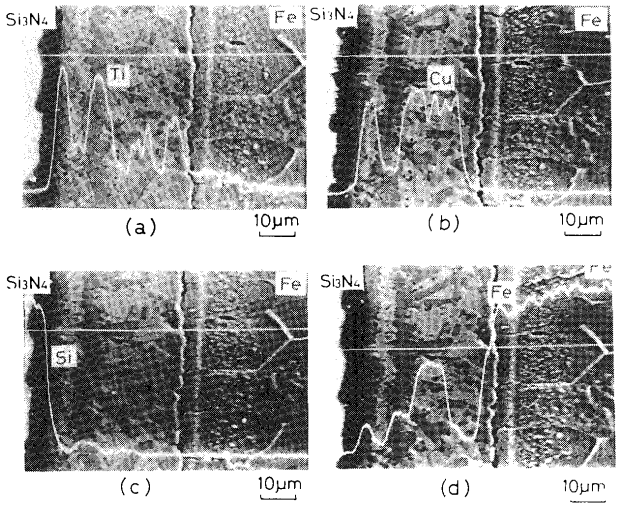

Fig. 7 Line analyses of Ti, Si, Cu and Fe in $Fe/Cu_{50}Ti_{50}/Si_3N_4$ joint.

In joining of Si_3N_4 to Kovar alloy as shown in **Fig. 9**, the decomposition of Si_3N_4 took place, similarly to the joining of Si_3N_4 to Fe, and Fe and Co dissolve into the filler from Kovar alloy. In joining of Si_3N_4 to Invar alloy the line analysis of Ti in **Fig. 10** shows the Ti rich layer in the filler on Si_3N_4 side. The X-ray diffraction patterns of interface in Cu-Ti drop on Si_3N_4, and also the fracture surface of Si_3N_4/Cu-Ti/Si_3N_4 joint[3),5)] show that Ti rich layer composed of Ti nitride and silicide (TiN and Ti_5Si_3 etc.). On Invar alloy side intermetallic compounds containing high Ti, Fe and Ni content are observed, and at the intermediate of the filler Cu rich phase is formed. In joining of Si_3N_4 to Cu in **Fig. 11**, large amounts of copper

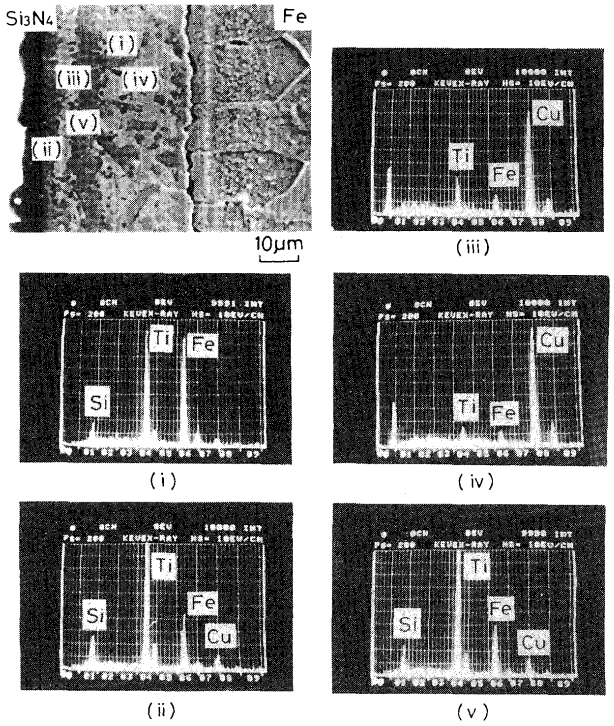

Fig. 8 Spot analyses of Ti, Si, Cu and Fe in $Fe/Cu_{50}Ti_{50}/Si_3N_4$ joint.

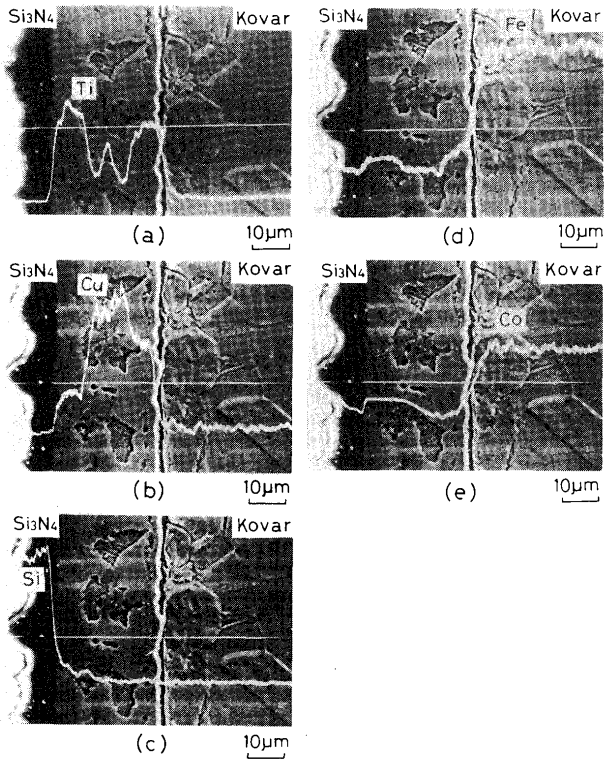

Fig. 9 Line analyses of Ti, Cu, Si, Fe and Co in Kovar alloy/$Cu_{50}Ti_{50}/Si_3N_4$ joint.

dissolve into the filler from copper, and the molten filler partly extends into copper, and the copper solid solution phase containing titanium re-precipites from the molten filler. This process results in that the interface between the filler and Cu is not clear, in comparison with other joints

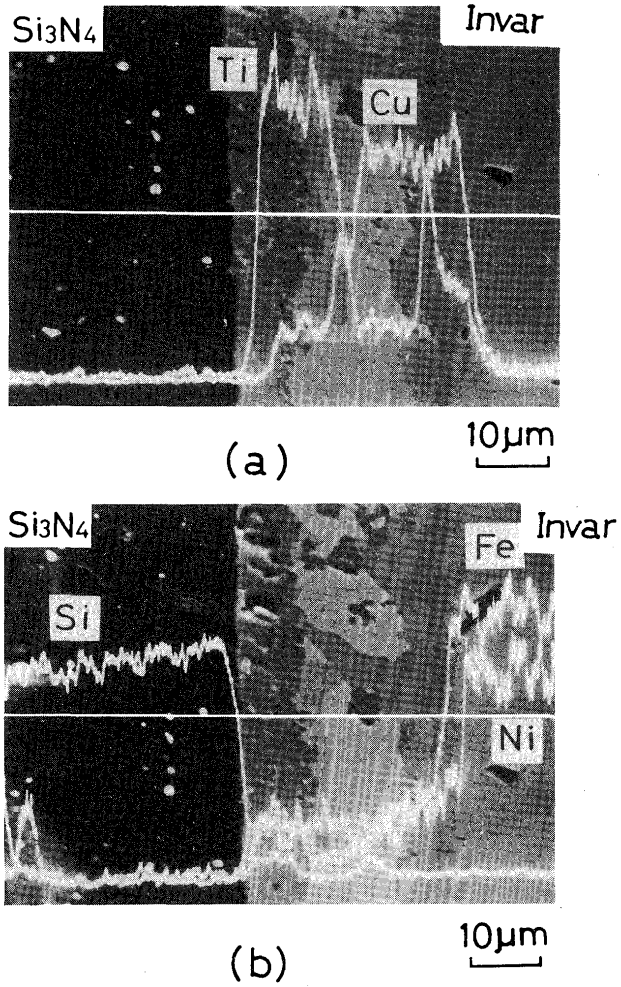

Fig 10 Line analyses of Ti, Si, Cu, Fe and Ni in Invar alloy/$Cu_{50}Ti_{50}/Si_3N_4$ joint.

in Figs. 8 to 10. In other words, Si_3N_4 joins to Cu by the isothermal solidification process. Further, similarly to the joining of Si_3N_4 to Fe, Si_3N_4 reacts with Ti in the filler.

4. Discussion

In joining of Si_3N_4 to metal such as Fe that possesses the large thermal expansion coefficient in **Fig. 12**, the difference of thermal expansion between Si_3N_4 and metal is attributable to the occurence of thermal stress that leads to the crack in Si_3N_4/metal joint. This type of crack is also observed in Si_3N_4/Cu and Si_3N_4/SUS304 joints. The stress distribution in ceramic/metal joint is further discussed.

The schematic distribution of thermal stress after joining is represented in **Fig. 13(a)**. (1) The stress distribution is discussed in two dimensional problem, and the ceramic is a half-infinite palte containing the section perpendicular to the joining interface, and the thickness of the ceramic is 1. (2) The uniform stress is applied to the joining interface of ceramic, and the direction of stress is centripetal, and pararell to the ceramic interface. In the case of that

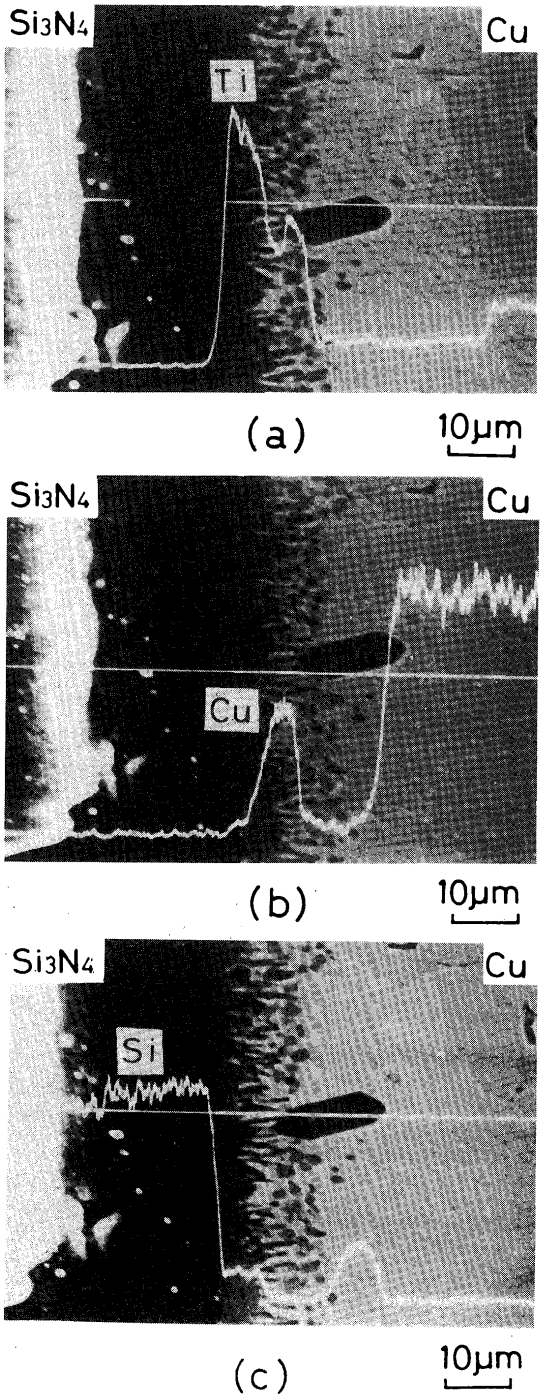

Fig. 11 Line analyses of Ti, Cu and Si in $Cu/Cu_{50}Ti_{50}/Si_3N_4$ joint.

the stress p kg/mm^2 is distributed in the joining part of 2c width, the stress distribution in ceramic is derived as follows.

The stress function ϕ is provided when the concentrated force P is applied in the positive y direction in **Fig. 13 (b)**[6].

$$\phi = -\frac{P}{\pi} r\theta \sin\theta \tag{1}$$

Fig. 12 Crack at Si_3N_4 in Fe/Si_3N_4 joint.

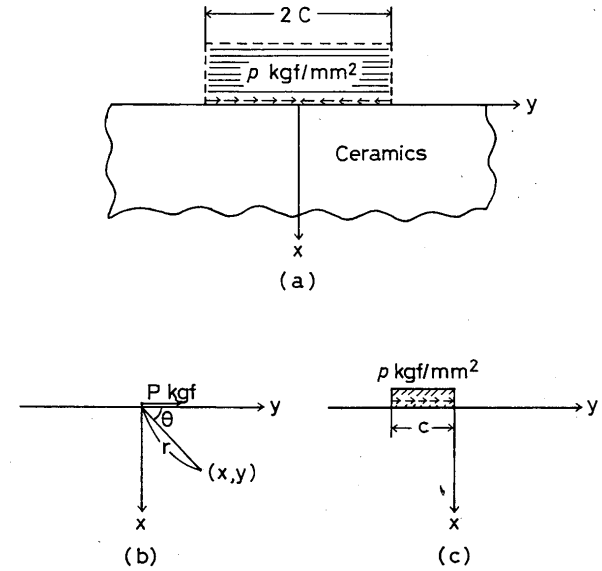

Fig. 13 Schematic of stress distribution in metal-ceramic joint: (a) stress distribution at interface of joint, (b) pole coordinates to calculate stress distribution, (c) integrated force at the interface of ceramic.

and

$$\sigma_r = \frac{1}{r}\frac{\partial\theta}{\partial r} + \frac{1}{r^2}\frac{\partial^2\theta}{\partial\theta^2} = -\frac{2}{\pi}\frac{\cos\theta}{r} \tag{2}$$

$$\sigma_\theta = \frac{\partial^2\phi}{\partial r^2} = 0 \tag{3}$$

$$\tau_{r\theta} = -\frac{\partial}{\partial}\left(\frac{1}{r}\frac{\partial\phi}{\partial\theta}\right) = 0 \tag{4}$$

When (r, θ) cordinates in (2), (3) and (4) are transformed to (x, y) cordinates,

$$\sigma_x = \sigma_r\cos^2\theta + \sigma_\theta\sin^2\theta - \tau_{r\theta}\sin\theta\cos\theta = -\frac{2P}{\pi}\frac{y^3}{(x^2+y^2)^2} \tag{5}$$

$$\sigma_y = \sigma_r\sin^2\theta + \sigma_\theta\cos^2\theta + 2\tau_{r\theta}\sin\theta\cos\theta = -\frac{2P}{\pi}\frac{x^2y}{(x^2+y^2)^2} \tag{6}$$

$$\tau_{xy} = (\sigma_r - \sigma_\theta)\sin\theta\cos\theta + \tau_{r\theta}(\cos^2\theta - \sin^2\theta) = -\frac{2P}{\pi}\frac{xy^2}{(x^2+y^2)^2} \tag{7}$$

When the distributed stress p instead of P is applied in the part of $y < 0$, σ_x, σ_y and τ_{xy} are derived by replacing P with $p$dy, and integrating from y to y + c.

$$\sigma_x = \int_y^{y+c} [-\frac{2p}{\pi}\frac{y^3}{(x^2+y^2)^2}]\,dy$$
$$= -\frac{p}{\pi}\left\{ln\frac{x^2+(y+c)^2}{x^2+y^2} + \frac{x^2}{x^2+(y+c)^2} - \frac{x^2}{x^2+y^2}\right\} \quad (8)$$

$$\sigma_y = \int_y^{y+c} [-\frac{2p}{\pi}\frac{x^2 y}{(x^2+y^2)^2}]\,dy$$
$$= \frac{p}{\pi}\left\{\frac{x^2}{x^2+(y+c)^2} - \frac{x^2}{x^2+y^2}\right\} \quad (9)$$

$$\tau_{xy} = \int_y^{y+c} [-\frac{2p}{\pi}\frac{xy^2}{(x^2+y^2)^2}]\,dy$$
$$= \frac{p}{\pi}\left\{\tan^{-1}(\frac{y}{x}) - \tan^{-1}(\frac{y+c}{x}) - \frac{xy}{x^2+y^2} + \frac{x(y+c)}{x^2+(y+c)^2}\right\} \quad (10)$$

When the distributed stress is applied in the part of y >0 in Fig. 13 (b).

$$\sigma_x = -\frac{p}{\pi}\left\{ln\frac{x^2}{x^2+y^2} + \frac{x^2}{x^2+(y-c)^2} - \frac{x^2}{x^2+y^2}\right\} \quad (11)$$

$$\sigma_y = -\frac{p}{\pi}\left\{\frac{x^2}{x^2+y^2} - \frac{x^2}{x^2+(y-c)^2}\right\} \quad (12)$$

$$\tau_{xy} = -\frac{p}{\pi}\tan^{-1}(\frac{-y}{x}) - \tan^{-1}(\frac{c-y}{x}) + \frac{xy}{x^2+y^2} + \frac{x(c-y)}{x^2+(c-y)^2} \quad (13)$$

The stress distribution in Fig. 13(a) is obtained by adding Eqs. 8 to 13.

$$\sigma_x = -\frac{p}{\pi}\left\{ln\frac{x^2+(y+c)^2}{x^2+y^2} + ln\frac{x^2+(y-c)^2}{x^2+y^2} + \frac{x^2}{x^2+(y+c)^2} + \frac{x^2}{x^2+(y-c)^2} - \frac{2x^2}{x^2+y^2}\right\} \quad (14)$$

$$\sigma_y = \frac{p}{\pi}\left\{\frac{x^2}{x^2+(y+c)^2} + \frac{x^2}{x^2+(y-c)^2} - \frac{2x^2}{x^2+y^2}\right\} \quad (15)$$

$$\tau_{xy} = \frac{p}{\pi}\left\{\tan^{-1}(\frac{y}{x}) - \tan^{-1}(\frac{-y}{x}) - \tan^{-1}(\frac{y+c}{x}) + \tan^{-1}(\frac{c-y}{x}) - \frac{2xy}{x^2+y^2} + \frac{x(c+y)}{x^2+(c+y)^2} - \frac{x(c-y)}{x^2+(c-y)^2}\right\} \quad (16)$$

The stress distribution in ceramic should be expressed by means of principal stresses σ_1, σ_2. The principal stresses (σ_1, σ_2) are given by the following equations.

$$\sigma_1 = \frac{1}{2}(\sigma_x+\sigma_y) + \frac{1}{2}\sqrt{(\sigma_x-\sigma_y)^2+4\tau_{xy}^2} \quad (17)$$

$$\sigma_2 = \frac{1}{2}(\sigma_x+\sigma_y) - \frac{1}{2}\sqrt{(\sigma_x-\sigma_y)^2+4\tau_{xy}^2} \quad (18)$$

Where the principal directions θ_1 and θ_2 of principal stresses σ_1 and σ_2 are given as follows,

$$\theta_1, \theta_2 = \frac{1}{2}\tan^{-1}\frac{2\tau_{xy}}{\sigma_x-\sigma_y} \quad (19)$$

The difference between θ_1 and θ_2 is $\pi/2$. The correspondence between the principal stresses (σ_1, σ_2) and the principal directions (θ_1, θ_2) is determined by the plus or minus sign of $d^2\sigma_n/d\theta^2$.

$$\frac{d^2\sigma_n}{d\theta^2} = 2(\sigma_y-\sigma_x)\cos 2\theta - 4\tau_{xy}\sin 2\theta \quad (20)$$

Therefore, θ_1 in $d^2\sigma_1/d\theta^2 < 0$ corresponds to σ_1, and θ_2 in $d^2\sigma_2/d\theta^2 > 0$ corresponds to σ_2. The principal stresses and the directions are derived from eqs. 14 to 20.

When the distributed stress is $p = 10$ kg/mm^2 which is relatively smaller than the yield stress of Fe and c = 3 mm that corresponds to the radius of metal in joining of Si_3N_4, the principal stresses and principal directions in ceramic are given in **Fig. 14**. The length and direction of arrow in the line show the magnitude of principal stress and direction of principal direction, respectively. The solid line and dotted line indicate the tension and compression stress, respecively. The stress distribution at $y > 0$ is shown in Fig. 14 since the distribution is symmetry against x cordinate. The σ_1 and σ_2 below 1 kg/mm^2 are omitted. The tension-tension area where both σ_1 and σ_2 are positive exists near the joining edge (y = 3 mm), and the compression-compression area in bell shape where both σ_1 and σ_2 are negative exists in the central part (y = 0) as shown in Fig. 14. The fairly large stresses perpendicular to the joining interface are calculated at the joining edge. The presence of the two areas is attributable to

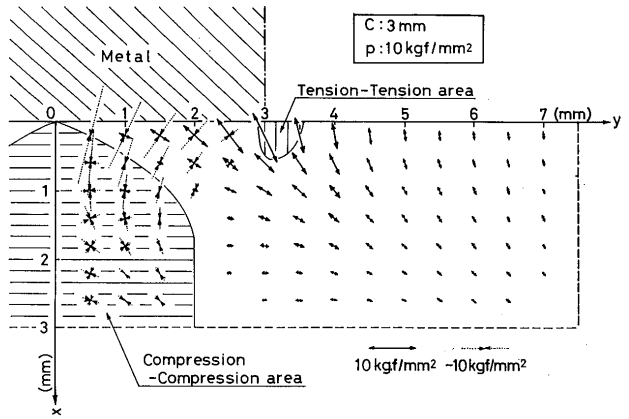

Fig. 14 Distribution of principal stress in metal-ceramic joint (c = 3 mm, p = 10 kg/mm^2).

the crack initiation near the joining edge and the crack stopping at the central part of ceramic in Fig. 12.

The similar stress distribution takes place in joining Si_3N_4 to oxide ceramics (Al_2O_3, ZrO_2 and MgO). The joints of Si_3N_4/oxide ceramics except for Al_2O_3 separate at the joining interface owing to the thermal stress on cooling after brazing. In Si_3N_4 joint the crack perpendicular to the joining interface is observed.

5. Conclusion

The joining of Si_3N_4 to metals and alloys was conducted, where Si_3N_4 attracts recent interests because of its superior mechanical properties. In order to apply the active metal brazing method, amorphous $Cu_{50}Ti_{50}$ filler about 1 cm wide and about 45 μm thick was produced by liquid quenching. Si_3N_4 was joined to Fe, Cu, Super Invar, Invar, Kovar and SUS304 using amorphous $Cu_{50}Ti_{50}$ filler at 1000°C for 5 min in vacuum.

During brazing Si_3N_4 reacts with Ti in Cu-Ti filler, and Fe, Cu or Co etc. dissolves into the filler from metals or alloys. In joining of Cu, large amounts of copper dissolve into the Cu-Ti filler and Ti in the filler diffuses into Cu.

The joining strength of Si_3N_4 to metals and alloys treands to decrease with an increase in the thermal expansion coefficient or the product of thermal expansion coefficient and elastic modulus of metals or alloys. This implies that the thermal stress arised from the difference between Si_3N_4 and metals (or alloys) during cooling affects the joining strength of joints. According to the elastic calculation, the tensile stress, that takes place in the tension-tension stress area and is perpendicular to the joining interface in ceramic near the interface, affects the joining strength of ceramic/metal or alloy joint.

References

1) M. Naka, K. Asami, I. Okamoto and Y. Arata, Trans. JWRI, 12 (1983), No. 2, 145.

2) M. Naka, K. Sampath, I. Okamoto and Y. Arata, Proc. Inter. Conf. Joining of Metals, ed by O. AL-Erhayen, Denmark, 1984, p 148.

3) M. Naka and I. Okamoto, J. High Temp. Soc., 11 (1985), 148.

4) L.F. Vitovitch, Handbook of Heat-resistant Compounds, Ni-so Tsushin Co., p 30.

5) M. Naka, T. Tanaka and I. Okamoto, Quarterly J. Japan Weld. Soc., to be published.

6) S. Timoshenko and J. Goodier, trans. by K. Kinta, Korona Co., 1971, p 99.

7) K. Terasawa and Y. Matsuura, Material Mechanics, vol. I, Kaibundo, 1974, p 17.